STM JOURNALS

Journal of
Polymer & Composites

ISSN: 2321-2810 (Online)
ISSN: 2321-8525 (Print)
Volume 11, Special Issue 2, 2023
DOI (Journal): 10.37591/JoPC

http://engineeringjournals.stmjournals.in/index.php/JoPC/index

Research JoPC

Influence of Crystallization Time by Hydrothermal Synthesis of Ag NPs-Zeolite Composite

Ruaa F. Ahmed[1,*], Mohamed K. Dhahir[2]

Abstract

The nanocomposites Ag NPs-zeolite involve zeolite loaded with silver nanoparticles and have been prepared by an easy one-pot hydrothermal autoclave method. Three samples of silver-bearing zeolite were prepared for 8 hours, 6 hours, and 4 hours, respectively, inside an autoclave at 100°C. A range of characterization procedures were used to examine the samples, such as x-ray diffraction (XRD), field emission scanning electron microscopy (FESEM), UV-visible spectroscopy, and zeta potential. Results proved that the Ag NPs-zeolite composite shows good distribution of silver nanoparticles in zeolite, and silver nanoparticles are stable inside the pores of zeolite, resulting in the formation of a core-shell with a crystalline structure; a longer crystallization time results in a highly crystalline phase with a larger average particle size and higher absorption intensity; and all samples exhibit high levels of absorption in the region of UV absorption. The composite has low stability of the Ag-zeolite nanoparticles, and the composite contains silver aggregation on the surface of the zeolite. The 8-hour sample is the best for applications. It can be used in the preparation of the photoanode pole in photoelectrochemical cells after deposition on fluorine-doped tin oxide as a thin film for renewable energy, catalytic, electrochemical, and anti-bacterial systems.

Keywords: Nanoparticles, silver, composites, zeolites, hydrothermal synthesis

INTRODUCTION

The importance of nanoparticles (NPs) and their use in a variety of industries has prompted several studies. In comparison to their bulk metal states, nanoscale metals exhibit distinct features. Transition metals stand out among the numerous NPs because of their unique physicochemical features [1].

Silver nanoparticles (Ag NPs) are transition metals due to their low electronic band gap, which promotes high activity under both ultraviolet (UV) and visible light via the surface plasmon resonance process and chemical stability in a variety of situations. They have gained a lot of attention as photocatalysts [2]. In particular, the catalytic properties of small noble metals depend on size, shape, structure, and composition, as well as their interaction with a support material. However, due to their quick aggregation, NPs' remarkable catalytic capacity may be swiftly lost. Finding a matrix system that serves as a host matrix for relatively small NPs and is characterized by high catalytic activity, selectivity, and stability has been difficult for decades. Due to their unique porous structure that regulates molecule transportation, acidity that encourages the adsorption of specific molecules to benefit the desired reaction, and high surface area for widespread metal NP distribution, zeolites are frequently used as support matrices for catalytic applications and adsorbents. The morphology, structure, and size distribution of zeolite have a strong influence on their chemical and physical properties, as well as their uses and properties [3, 4].

***Author for Correspondence**
Ruaa F. Ahmed
E-mail: ruaafawzi87@gmail.com

[1]Student, Institute of Laser for Postgraduate Studies, University of Baghdad, Baghdad, Iraq
[2]Asstistant Professor. Dr, Institute of Laser for Postgraduate Studies, University of Baghdad, Baghdad, Iraq

Received Date: December 08, 2022
Accepted Date: January 31, 2023
Published Date: April 18, 2023

Citation: Ruaa F. Ahmed, Mohamed K. Dhahir. Influence of Crystallization Time by Hydrothermal Synthesis of Ag NPs-Zeolite Composite. Journal of Polymer & Composites. 2023; 11(Special Issue 2): S80–S90.

Zeolite, an alkali/alkaline-earth metal hydrated aluminosilicate mineral, has received a lot of attention lately as a readily accessible and affordable natural mineral. $[A1O_4]^{5-}$ and $[SiO_4]^{4-}$ units are joined by sharing an oxygen atom and their crystal structure. In cavities within the crystal structure of zeolite, Na^+, K^+, and Ca^{2+} cations are also typically present. The uniform presence of channels and pores in zeolite is a significant benefit. Due to its high surface-to-volume ratio, zeolite is considered to have a strong capacity for absorption. As a result, zeolite's surface absorption is greatly improved, and the bonding/anchoring of nano-sized particles to its surface is also improved [5]. because of their well-defined pore and channel architectures. These materials are commonly utilized as ion exchangers, catalysts, and adsorbents in industry. Photocatalysis, electrochemistry applications, antibacterial agents, and oxidation processes have all been reported to be active with silver-based zeolites [6]. A diverse class of materials is called silver-zeolite composites. Their uses include pressure or chemical sensors, information storage, antimicrobial materials, catalysts, and more. Zeolites are used as molecular scaffolds in the manufacturing of luminous materials with transition metal oxide [7]. More recent research has focused on synthetic and natural zeolites as well as composites including metal(s) or metal oxide(s) nanoparticles (NPs) or a mixture of the two, expanding the application sectors. Among the metal and metal-oxide-containing composites described, silver and silver oxide NPs, including zeolite nanocomposites, are of special interest [8].

In general, there are many methods to load metals on boost materials, such as ion-exchange and hydrothermal methods [9], or by exchange cation [10, 11]. The zeolite structure can be filled with transition metal atoms through conventional impregnation, hydrothermal processes, photosynthesis, or cation exchange using a traditional ion-exchange approach. These can be developed more easily if a one-pot hydrothermal process is investigated. Recently, researchers' interest in the single-pot hydrothermal approach has increased [6]. The process of hydrothermal synthesis is used to create materials at low temperatures with high vapor pressure. This approach is thought to be the most energy-efficient and environmentally benign because the reaction is carried out under closed-system settings. Typically, hydrothermal synthesis is performed in aqueous solutions using a Teflon-lined stainless steel autoclave [12].

In this paper, the effect of changing the crystallization time on the nano silver compound loaded on the nano-zeolite for three samples was studied by a hydrothermal autoclave method, and then the structure and morphology characterization were found. A comparison between the samples was done to choose which one is better in applications of catalyst.

MATERIALS AND METHODS

Materials

Zeolite particle size of 50 nm. Specific surface area (SSA) 340 m^2/g, silver nanoparticles Ag 20 nm, spherical, Hongwu International Group Ltd. – China, deionized water, PEG600 Mfg. (Alpha Chemika made in India), and absolute ethyl alcohol (Alpha Chemika, India), was used to prepare an Ag NPs-zeolite composite.

Preparation of Ag NPs-Zeolite Composite

The Ag NPs-zeolite composite was synthesized by the hydrothermal method wherein silver nanoparticles (0.2 g) were dissolved in deionized water (5 mL) with (10 mL) of PEG600 at 25°C for 30 minutes with stirring, and then 0.2 g of nano zeolite with absolute ethyl alcohol (20 mL) was added step by step to the mixture with stirring for 2 hours.

Finally, the crystallization method was easy; the mixture was placed inside a hydrothermal autoclave, and then a thermal oven that was kept at 100°C for 8, 6, and 4 hours for three samples, respectively, as shown in Figure 1.

The Ag NPs-zeolite composite was obtained after steps of filtration and drying at 100°C for 1 hour in the oven, with the pH kept near neutral during the step of the filtration process as shown in Figure 1.

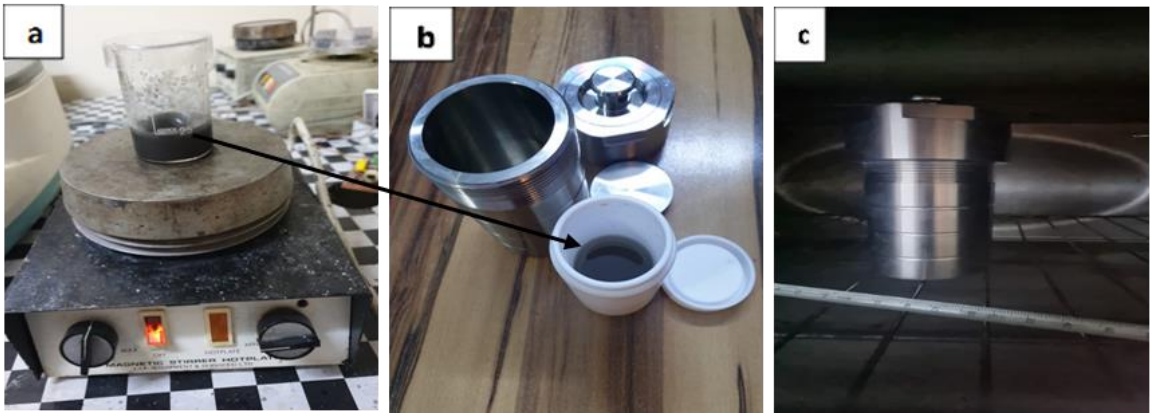

Figure 1. Preparation of silver-loaded zeolite composite steps (a) Ag (NP)-zeolite for 2 hours in a stirrer (b), the mixture in a Teflon cup (c), autoclave in a 100°C thermal oven.

Characterization

The X-ray diffraction (XRD-6000) Shimadzu 220V/50 Hz (Japan) patterns of the samples were recorded using a diffractometer operating with a Cu-Kα radiation in the 2θ angle range 5° to 80° with a step of 0.05° and with 0.60 s of accumulation at each point. Field emission scanning electron microscope (FESEM) (FEI Japan) was used to determine the morphology and particle size of Ag (NP)-zeolite. Fourier-transform infrared (FTIR) spectrum was recorded on a Shimadzu 8300/8700 in the region of 4000–400 cm^{-1}. The Shimadzu UV-VIS-NIR 1800, 240V (Japan) spectrophotometer was obtained as previously described [13]. Using a UV-visible spectrometer, the spectra between 190 and 1100 nm were captured.

RESULTS AND DISCUSSION

X-Ray Diffraction Studies

XRD patterns of the Ag NPs-zeolite composite are shown in Figure 2. The purpose of the XRD investigation was to learn more about the crystalline nature of the nanocomposites synthesized. The good crystalline quality of the produced samples is confirmed by the sharp peaks [14]. The absorption peaks for zeolite appeared at 2θ = 13.1°, 22.4°, 23.1°, 26.5° and 27.1° All of the zeolites' diffraction patterns clearly correspond to those on the zeolite standard card (JCPDS39-0223). From Figure 2, it is evident that the zeolite is crystalline. Also it is observed that the Ag NPs-zeolite composite has notable peaks around 2θ = 38.6°, 44.7°, 64.9°, and 77.8^0, which correspond to the (111), (200), (220), and (311) crystal planes. These peaks' development shows that the crystalline phase of silver has developed within the zeolite framework, which, when matched with standard silver values (JCPDS 04–0783), can be indexed using the facets of silver's face-centered cubic crystal structure. These peak heights are consistent with earlier reports [15, 16]. Figure 2 shows that the crystallinity of the sample increases with aging time. The aging process allows for crystal size regulation. The production of impurity phases is reduced, and crystallization is accelerated according to Nazir et al. [17]. So the longer crystallization time of the composition of Ag NPs-zeolite produced a highly crystalline phase, as evidenced by the XRD peak intensity of the 8-hour sample, more desirable in comparison with samples at 6 and 4 hours.

FESEM Analysis

Figure 3 shows the FESEM images for zeolite and Ag NPs-zeolite composite. The morphology appears in Figure 3a for the surface of zeolite in the form of flakes, and their size ranges from 43 to 50 nm. According to Das et al. [18], the morphology of the composite for three samples shows a good distribution of silver nanoparticles in zeolite. Silver nanoparticles are stable inside the pores of zeolite and this is called core-shell structure, as shown in Figure 3c. A 4-hour sample is shown in Figure 3b with particle size ranging between 88 and 183 nm, a 6-hour sample with particle size ranging between 46 and 143 nm is shown in Figure 3c, and an 8-hour sample with particle size ranging between 56 and 193 nm in is shown in Figure 3d. Figure 3e shows that the longer the crystallization time, the larger the average particle size. This means that the higher the crystallization time, Ag NPs-zeolite composite may

contain metallic particles,which begin to enlarge clearly after aging for 6 and 8 hours, which agrees with previous research [19]. The composite displayed a rough surface with a spherical structure for silver nanoparticles and showed many silver clusters. At 100°C to 200°C, reduction results in the creation of silver clusters on the surface of zeolite. This agrees with previous research [20]. Also, some shiny places corresponding to the AgNPs appeared on the surface of the zeolite nanoparticle; therefore, the AgNPs were rather well distributed in the zeolite nanoparticles. It was supported by form (a) Ag-Zeo from Mintcheva et al. [21].

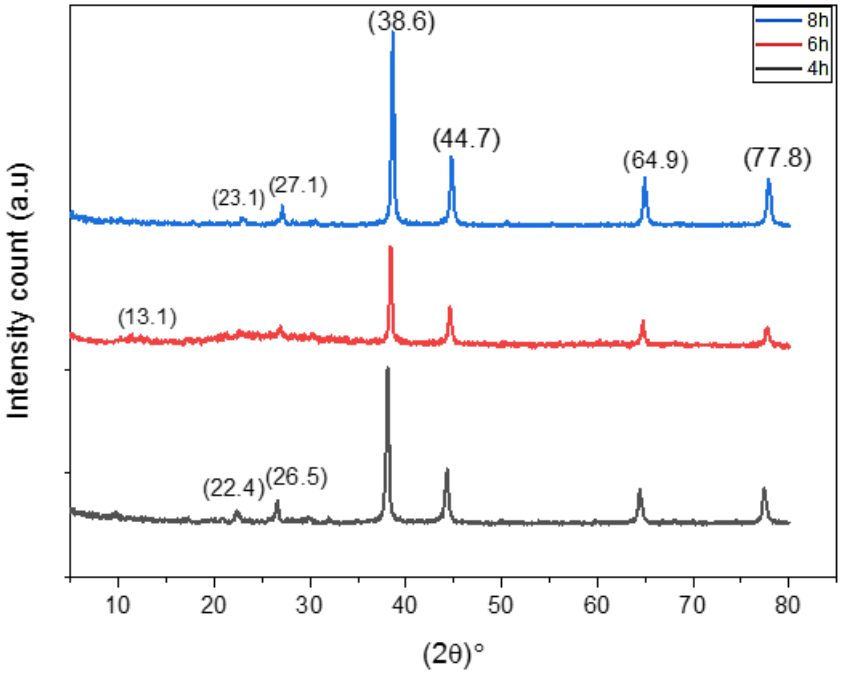

Figure 2. X-ray diffraction (XRD) patterns Ag NPs-zeolite composite for three samples.

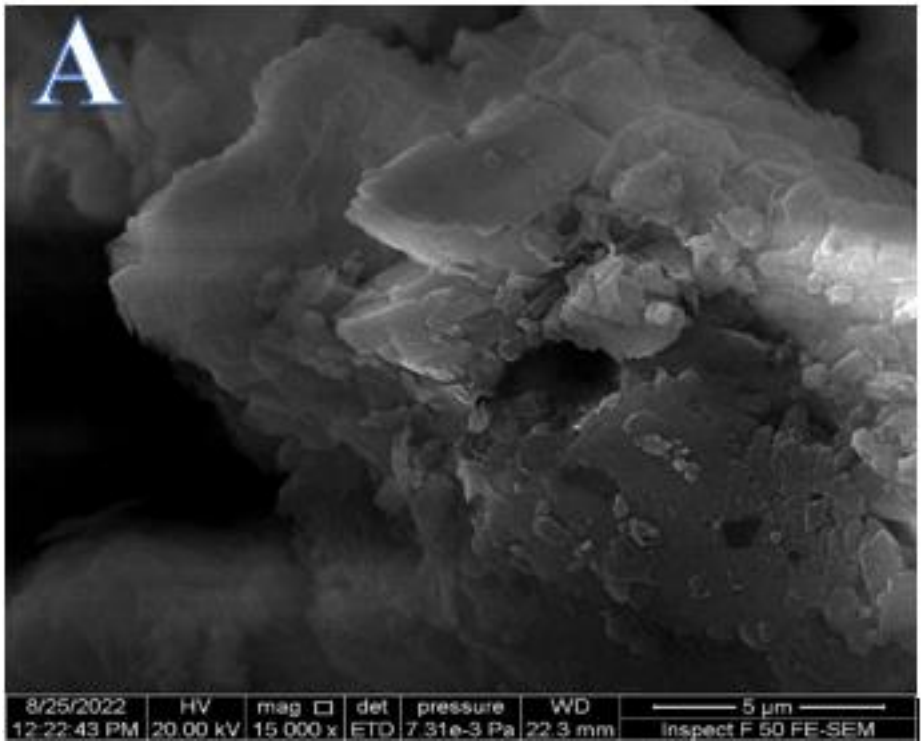

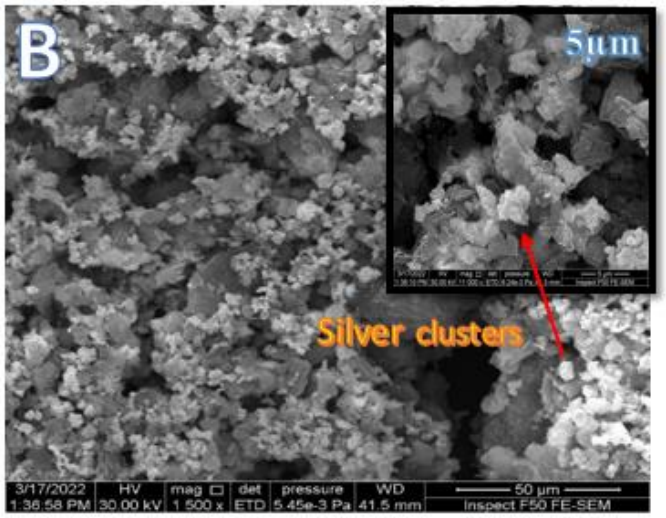

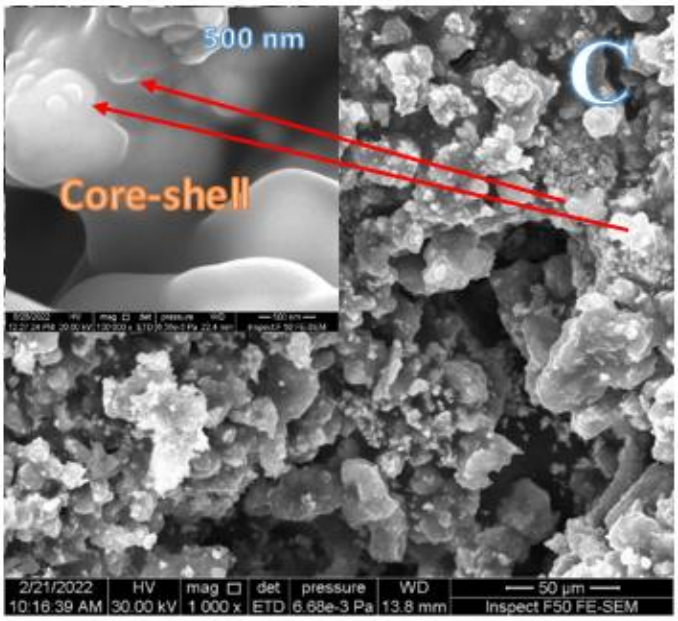

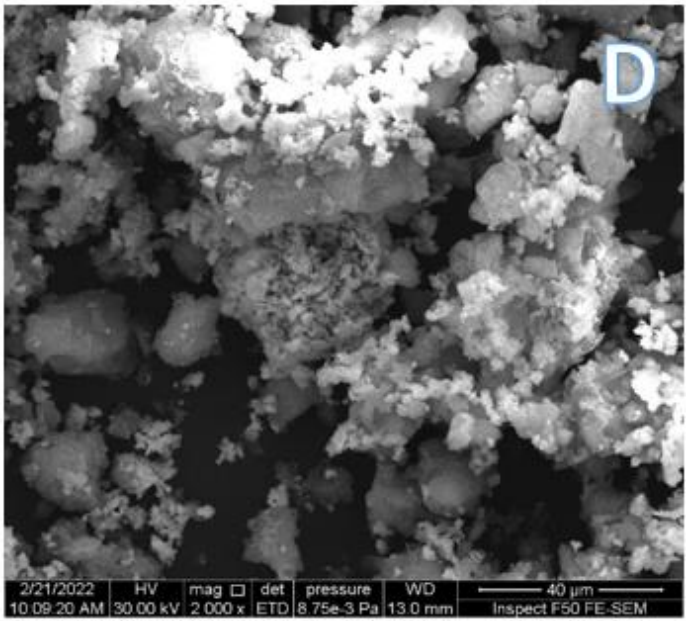

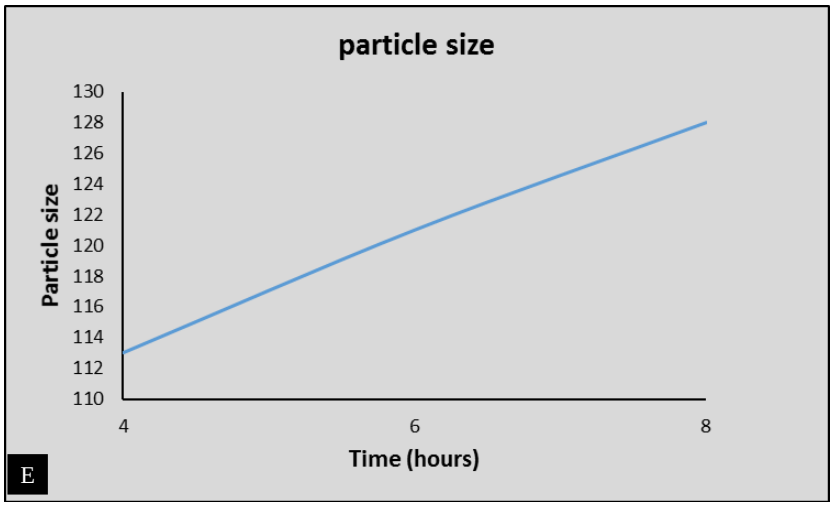

Figure 3. Field emission scanning electron microscopy (FESEM) images for zeolite and Ag NPs-zeolite composite for three samples: (a) zeolite, (b) a 4-hour sample, (c) a 6-hour sample, (d) an 8-hour sample, and (e) the average particle size for three samples.

UV-Visible Spectral Study

All samples exhibit a high level of absorption in the region of UV absorption. Figure 4a for zeolite shows the highest peak of absorption appears at the peaks 248 and 288 nm, Figure 4b for silver shows the highest peak at 284 nm. Ag species with more Ag atoms often produce UV-Vis bands at a longer wavelength, and the bands at 260 and 284 nm are attributed to Ag_n δ+ (n = 4–8) clusters. This is in agreement with earlier research [13, 22]. The reflectance spectra of the materials used Ag NPs-zeolite composite in the visible and ultraviolet range were recorded. Below 300 nm, non-exchanged zeolites were observed. The silver-loaded zeolites produced stronger signals in the UV range (200–300 nm).

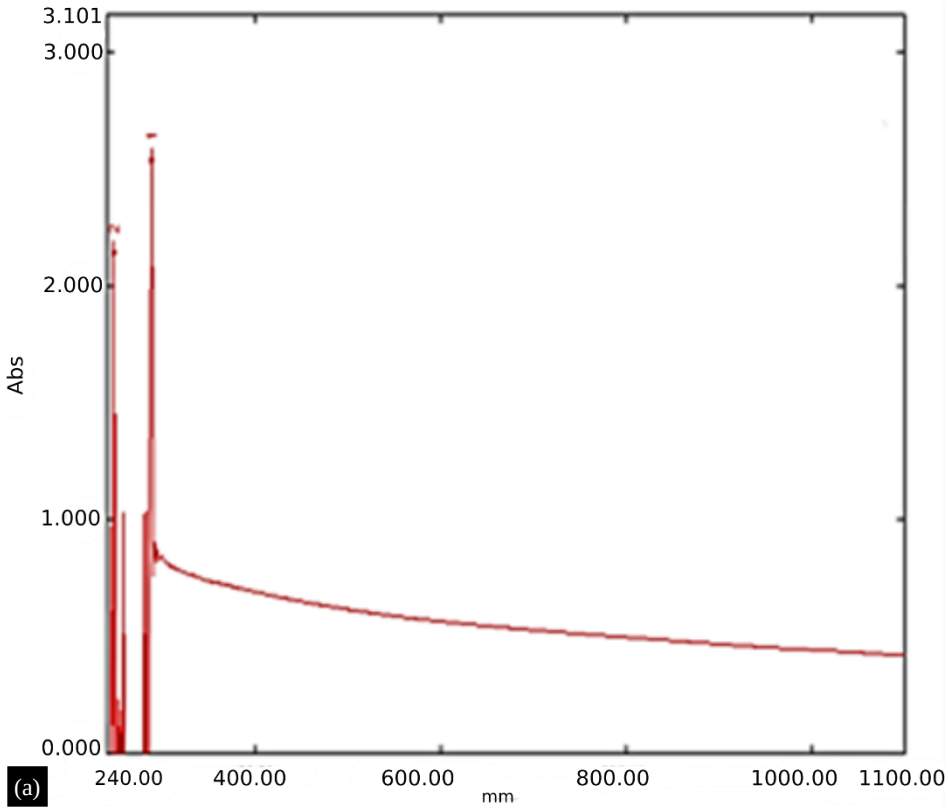

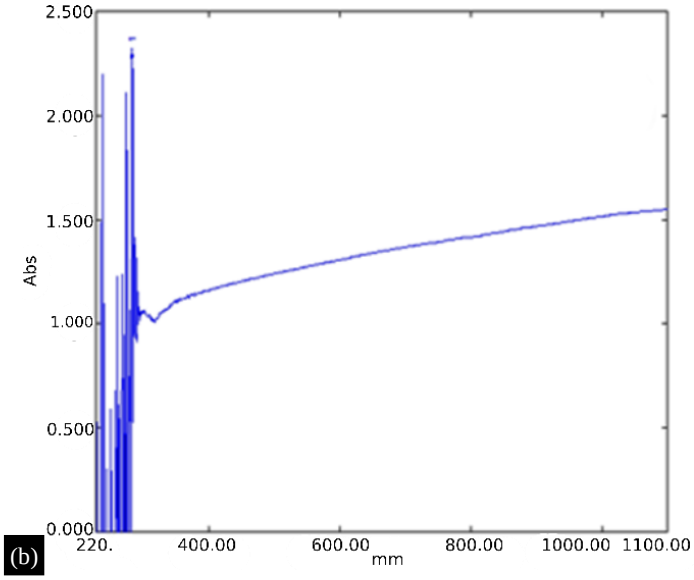

(b)

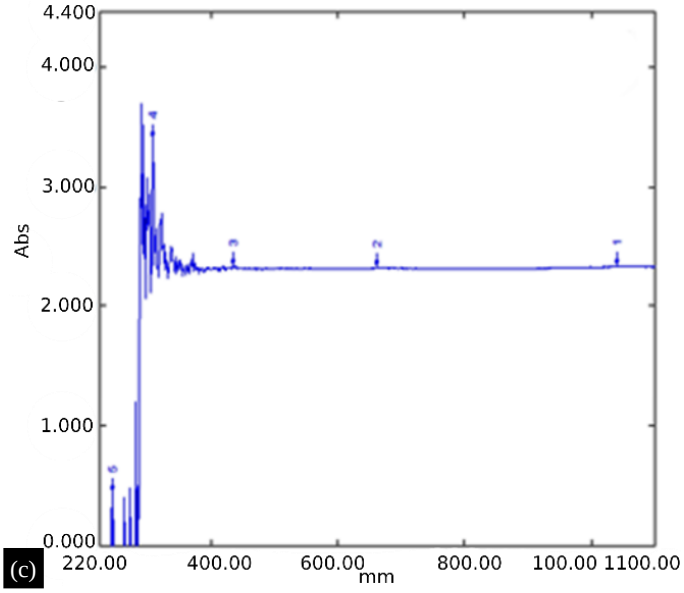

(c)

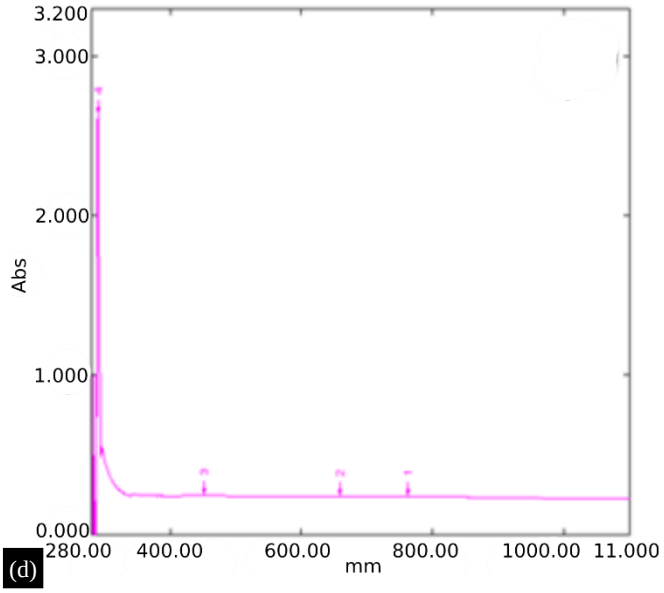

(d)

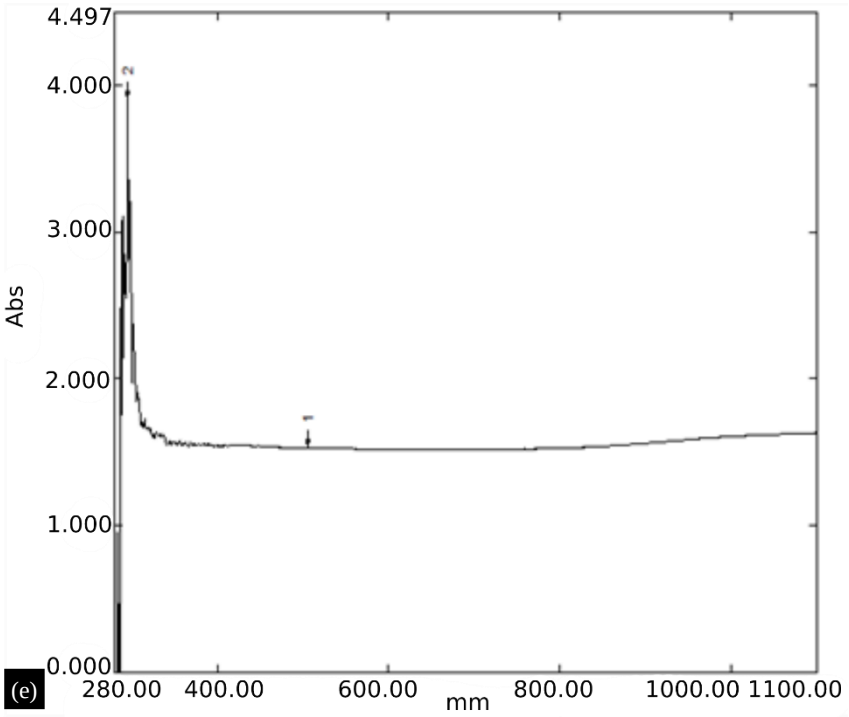

Figure 4. UV-Visible spectrum for zeolite, silver NPs and Ag NPs-zeolite composite for three samples (a) zeolite, (b) silver (Ag NPs), (c) 4-hours sample, (d) 6-hour sample, (e) 8-hour sample.

These signals have previously been linked to isolated silver ions that are present at particular locations within the zeolite framework. It also shows that the intercalation of silver ions into the zeolite structure has altered the zeolite's electron structure. which is well in line with other reports [19, 23]. Figure 4 shows absorption peaks for Ag NPs-zeolite composite for three samples: 4-hour (c), 6-hour (d), and 8-hour (e) respectively at 309 and 245 nm, 452 and 290 nm, and 505 and 296 nm, respectively. The process of prolonging the crystallization time increases the intensity of the absorption, as shown in the 8-hour sample in Figure 4e indicating the growth of the amount of metal Ag particles according to Temerev et al. [19]; this is what was shown by the Figure 3e. This explains the shifting of wavelengths of the three samples from the UV region to the visible, depending on the particle size, which increases due to the increase in silver clusters with the increase in the crystallization time.

Zeta Potential Analysis

The surface charge of the Ag NPs-zeolite composite dissolved by the solvent solution after the crystallization process by hydrothermal autoclave to obtain the Ag NPs-zeolite core-shell was measured by zeta-potential. Zeta potential was typically used to gauge a surface's resistance to agglomeration. The stability of an Ag NPs-zeolite composite in colloidal form can be predicted using the zeta potential, with a value of greater than +30 mV or less than –30 mV suggesting the least amount of particle aggregation brought on by electrostatic attraction. Where the electrical stability of colloids increases when their zeta potentials, whether negative or positive, are enhanced, whereas aggregates and agglomerates are described by low zeta potential values, it was supported by earlier studies [24, 25]. The surface charge for zeta potential for the Ag NPs-zeolite composite is illustrated in Figure 5. It has low stability of the Ag-zeolite nanoparticles, mobility values, and zeta potential values for three samples observed in the Table 1. This explains the presence of silver nanoclusters on the surface of the zeolite in the above FESEM images.

Table 1. The values of the zeta potential and the mobility of the Ag-zeolite) nanoparticle solution

The nano particle solution	Zeta potential (mV)	The mobility ($m^2 V^{-1} s^{-1}$)
Ag-zeolite	-25.01	-1.95

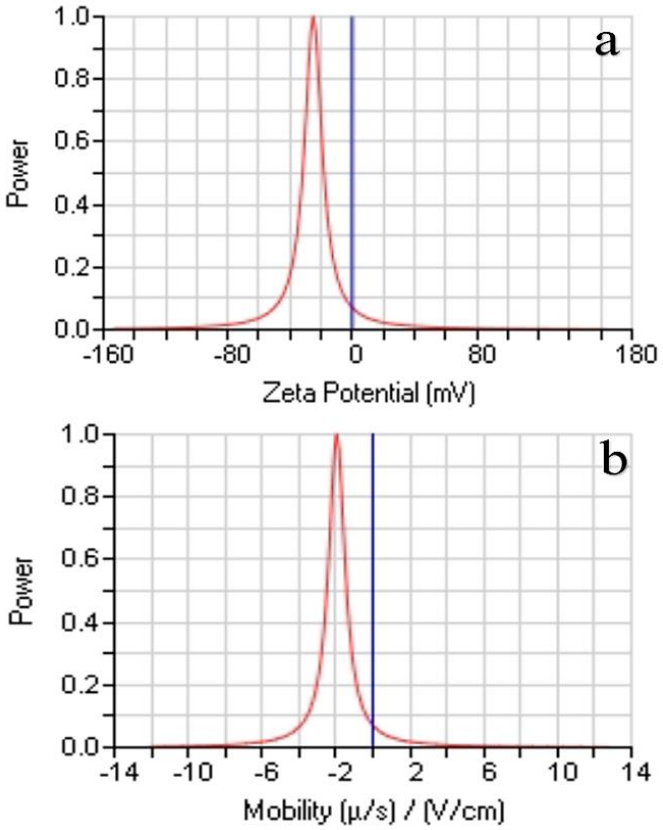

Figure 5. (a) The Ag-zeolite nanoparticle solution's zeta potential (mV); (b) the Ag-zeolite nanoparticle solution's mobility ($m^2 V^{-1} s^{-1}$).

CONCLUSIONS

In this paper, a hydrothermal method at 100°C was used to synthesize an Ag NPs-zeolite composite, which is an effective method in the manufacture and loading of noble elements. Silver nanoparticles were successfully loaded into the pores and on the surface of the zeolite. The characterization tests conducted on the samples were XRD, FESEM, UV-Visible, and Zeta potential. The results of the examinations indicated that the sample after 8 hours is more crystallized and has a higher intensity of absorption, but with the increase in the crystallization time, the particle size average increases gradually, so it can be used in different applications such as catalysts, antimicrobial materials, and others [6].

REFERENCES

1. Shameli K, Ahmad MB, Zargar M, Yunis WM, Ibrahim NA. Fabrication of silver nanoparticles doped in the zeolite framework and antibacterial activity. Int J Nano Med. 2011; 6: 331–341.
2. Zhou R, Srinivasan MP. Photocatalysis in a packed bed: degradation of organic dyes by immobilized silver nanoparticles. J Environ Chem Eng. 2015; 3 (2): 609-616.
3. Horta-Fraijo P, Smolentseva E, Simakov A, José-Yacaman M, Acosta B. Ag nanoparticles in A4 zeolite as efficient catalysts for the 4-nitrophenol reduction. Microporous Mesoporous Mater. 2021; 312: 110707.
4. Pangan N, Gallardo S, Gaspillo PA, Kurniawan W, Hinode H, Promentilla M. Hydrothermal synthesis and characterization of zeolite A from corn (*Zea mays*) stover ash. Materials. 2021; 14 (17): 4915.
5. Torkian N, Bahrami A, Hosseini-Abari A, Momeni MM, Abdolkarimi-Mahabadi M, Bayat A, Hajipour P, Rourani HA, Abbasi MS, Torkian S, Wen Y. Synthesis and characterization of Ag-ion-exchanged zeolite/TiO_2 nanocomposites for antibacterial applications and photocatalytic degradation of antibiotics. Environ Res. 2022; 207: 112157.
6. Hu X, Bai J, Wang J, Li C, Xu W. Preparation of 4A-zeolite-based Ag nanoparticle composite

catalyst and research of the catalytic properties. RSC Adv. 2015; 5 (4): 2968–2973.
7. Coutino-Gonzalez E, Roeffaers MB, Dieu B, De Cremer G, Leyre S, Hanselaer P, Fyen W, Sels B, Hofkens J. Determination and optimization of the luminescence external quantum efficiency of silver-clusters zeolite composites. J Phys Chem C. 2013; 117 (14): 6998–7004.
8. Tauanov Z, Shah D, Inglezakis V, Jamwal PK. Hydrothermal synthesis of zeolite production from coal fly ash: a heuristic approach and its optimization for system identification of conversion. J Cleaner Prod. 2018; 182: 616–623.
9. Shi Y, Ye S, Liao H, Liu J, Wang D. Formation of luminescent silver-clusters and efficient energy transfer to Eu^{3+} in faujasite NaX zeolite. J Solid State Chem. 2020; 285: 121227.
10. Wattanawong N, Chatchaipaiboon K, Sreekirin N, Aht-Ong D. Fabrication of poly (butylene succinate) composite films with silver doped ZSM-5: effect of silver ZSM-5 on antibacterial activity and biodegradable behavior. Mater Sci Forum. 2020; 990: 256–261).
11. Coutino-Gonzalez E, Roeffaers MB, Dieu B, De Cremer G, Leyre S, Hanselaer P, Fyen W, Sels B, Hofkens J. Determination and optimization of the luminescence external quantum efficiency of silver-clusters zeolite composites. J Phys Chem C. 2013; 117 (14): 6998–7004.
12. Hussain SA, Muhammad SK, Alkhayatt AH. Hydrothermally growth of TiO_2 nanorods, characterization and annealing temperature effect. Kuwait J Sci. 2021; 48 (3): 1–10.
13. Temerev VL, Vedyagin AA, Iost KN, Pirutko LV, Cherepanova SV, Kenzhin RM, Stoyanovskii VO, Trenikhin MV, Shlyapin DA. Purification of exhaust gases from gasoline engine using adsorption-catalytic systems. Part 1: trapping of hydrocarbons by Ag-modified ZSM-5. Reaction Kinet Mechanisms Catal. 2019; 127 (2): 945–959.
14. Salem MA, Elsharkawy RG, Ayad MI, Elgendy MY. Silver nanoparticles deposition on silica, magnetite, and alumina surfaces for effective removal of Allura red from aqueous solutions. J Sol-Gel Sci Technol. 2019; 91 (3): 523–538.
15. Sowmyya T, Lakshmi GV. *Soymida febrifuga* aqueous root extract maneuvered silver nanoparticles as mercury nano sensor and potential microbicide. World Sci News. 2018; 114: 84–105.
16. Hamid MK, Ghafoor DA, Obaid SA. Characteristic and anticancer activity of silver nanoparticles of graviola (annona) fruit juice as a reducing agent. Arch Biochem Biophys. 2021; 21 (1): 1003–1010.
17. Nazir LS, Yeong YF, Sabdin S. Formation of pure NaX zeolite: effect of ageing and hydrothermal synthesis parameters. IOP Conf Ser Mater Sci Eng. 2018; 458 (1): 012002.
18. Das S, Pérez-Ramírez J, Gong J, Dewangan N, Hidajat K, Gates BC, Kawi S. Core–shell structured catalysts for thermocatalytic, photocatalytic, and electrocatalytic conversion of CO_2. Chem Soc Rev. 2020; 49 (10): 2937-3004.
19. Temerev VL, Vedyagin AA, Iost KN, Afonasenko T, Tsyrulnikov P. Enhanced adsorption properties of Ag-loaded β-zeolite towards toluene. Mater Sci Forum. 2018; 917: 180–184.
20. Lopes CW, Martinez-Ortigosa J, Góra-Marek K, Tarach K, Vidal-Moya JA, Palomares AE, Agostini G, Blasco T, Rey F. Zeolite-driven Ag species during redox treatments and catalytic implications for SCO of NH 3. J Mater Chem A. 2021; 9 (48): 27448–27458.
21. Mintcheva N, Panayotova M, Gicheva G, Gemishev O, Tyuliev G. Effect of exchangeable ions in natural and modified zeolites on Ag content, Ag nanoparticle formation and their antibacterial activity. Materials. 2021; 14 (15): 4153.
22. Shimizu K, Sawabe K, Satsuma A. Unique catalytic features of Ag nanoclusters for selective NOx reduction and green chemical reactions. Catal Sci Technol. 2011; 1 (3): 331–341.
23. Mazzocut A, Coutino-Gonzalez E, Baekelant W, Sels B, Hofkens J, Vosch T. Fabrication of silver nanoparticles with limited size distribution on TiO_2 containing zeolites. Phys Chem Chem Phys. 2014; 16 (35): 18690–18693.
24. Inbaraj BS, Chen BY, Liao CW, Chen BH. Green synthesis, characterization and evaluation of catalytic and antibacterial activities of chitosan, glycol chitosan and poly (γ-glutamic acid) capped

gold nanoparticles. Int J Biol Macromol. 2020; 161: 1484–1495.
25. Yahiya LZ, Dhahir MK, Faris RA. Novel and low-cost synthesis of ZnO nanorod coated by graphene oxide for enhanced physical absorption of ZNR from UV to VIS-IR region. Plant Arch. 2020; 20 (2): 1005–1008.

